Influence of radiation heat transfer during a Severe Accident

R.-I. Cázares-Ramírez
Posgrado en Energía y Medio Ambiente
División de CBI y CBS, UAM-Iztapalapa, 09340, Ciudad de México.
ricardo-cazares@hotmail.com

Gilberto Espinosa-Paredes*
Área de Ingeniería en Recursos Energético, UAM-Iztapalapa, 09340, México D.F.
**Sabático en la Facultad de Ingeniería de la Universidad Nacional Autónoma de México a través del Programa de Estancias Sabáticas del CONACyT*
gepe@xanum.uam.mx

J.-R. Varela-Ham, A. Vázquez-Rodríguez
Departamento de Ingeniería de Procesos e Hidráulica,
UAM-Iztapalapa, 09340, Ciudad de México.
jrvh@xanum.uam.mx; vara@xanum.uam.mx

M.-A. Polo-Labarrios
Comisión Nacional de Seguridad Nuclear y Salvaguardias
Doctor Barragán 779, Col. Narvarte, Ciudad de México, 03020, MEXICO
antonio.polo@cnsns.gob.mx

Abstract

The aim of this work is observe the influence of the radiation heat transfer during a severe accident of a BWR nuclear power plant. The analysis considers the radiation heat transfer in a participating medium. We consider the steam water as an isothermal gray gas, and the boundaries of the system as a gray diffuse isothermal surface for the clad and refractory surfaces for the rest, and consider an enclosure system. During a severe accident, starts the generation and the diffusion of hydrogen, but this element do not participate in the radiation heat transfer because have not radiation properties. The heat transfer process in the fuel assembly is considered with a reduced order model, and from this, we calculated and introduce the convection and the radiation heat transfer in the system. In this paper, we calculated and analyzed the system with and without the radiation heat transfer term in order to obtain the influence of the radiation heat transfer. We show the behavior of radiation heat transfer effects on the temporal evolution of the distributions of hydrogen concentration and temperature profiles in a fuel assembly where a stream of steam is flowing. Finally, this study can support to complement and make more accurate the model to analysis a severe accident.

1. INTRODUCTION

The behavior of a LWR fuel high temperature oxidation of Zircalloy-4 (Zry-4) cladding material in steam has been extensively studied for decades, whether in gaseous medium with air, oxygen or steam [1-7]. Those studies showed that Zry-4 oxidation by air has similarities with oxidation in steam due to the common reaction partner oxygen, and also important differences. The exothermal heat released during air oxidation is around 1.8 times higher than steam, which causes a higher rise rate temperature [6]. A large review on Zry-4 fuel cladding behavior in a loss-of-coolant accident was studied the chemical reactions between reactor zirconium alloy cladding and high temperature steam during a topical subject in the severe accident program for long time reported [8-9].

In the last decade has had a higher interest in the phenomena during a hypothetical severe nuclear accident and it was intensified by the Fukushima Daiichi station blackout accident. Assessment studies on the unit 1-3 of the possible core/vessel damage states were started [10-17].

The rest of this paper is organized as follows: in Section 2 the main heat radiation concepts for the analysis is introduced. In Section 3, the mathematical model is presented. In Section 4, the numerical solution is presented. In Section 5, the numerical experiment and the discussions of results are presented. Last, in Section 6, our conclusions are presented.

2. MAIN HEAT RADIATION CONCEPTS

The typical problems of heat transfer radiation in a system are solved by the classical model for radiation heat transfer that use the temperature of the system, the view factor and other optical parameters and do not considers the medium as a participating medium. In this paper we consider the steam water as a participating medium in the radiation heat transfer, and in the follow explain his properties, and effect in the analysis.

3.1. Gas Radiation Properties

A volume of gases can emit and absorb energy at a given temperature and pressure. The combustion products as the CO_2, steam, CO, NO, and NH_3, have radiation properties but air, helium, and hydrogen have no radiation properties (transparent to radiation). In general, gas emissivity and absorptivity increase with pressure and volumen, but decrease with temperature; gas emissity and absorptivity vary with wavelength. Under gray gas assumption, absortivity can be equivalent to emissity.

In general, gas emissity and absortivity are relatively low, approximately equivalent to an order of magnitude 0.1[18].

$$e_w = e_w\left(P_w L, T_g\right) @ 0.1 \tag{1}$$

3.2. Volumetric Absorption

Consider radiation heat transfer in a cavity filled with gas at a uniform temperature T_g. Spectral radiation absortion in a gas in proportional to the absortion coefficient $k_\lambda \left(1/m\right)$ and the thickness L of the gas. The radiation intensity decreases with increasing distance due to absorption.

$$dI_\lambda \left(x\right) = - k_\lambda I_\lambda \left(x\right) dx \tag{2}$$

$$\frac{dI_\lambda \left(x\right)}{I_\lambda \left(x\right)} = - k_\lambda dx \tag{3}$$

If k_λ is a constant value for a given gas, performing integration, we obtain

$$\ln I_\lambda \left(x\right) = - k_\lambda x + C_1 \tag{4}$$

$$I_\lambda \left(x\right) = e^{\left(- k_\lambda x + C_1\right)} = Ce^{- k_\lambda x} \qquad \text{at x=0, C=} I_{\lambda ,0} \tag{5}$$

$$I_\lambda \left(x\right) = I_{\lambda ,0} e^{- k_\lambda x} \qquad \text{at x=L} \tag{6}$$

$$I_{\lambda ,L} = I_{\lambda ,0} e^{- k_\lambda L} \tag{7}$$

This exponential decay is called Beer´s law. One can define the transmisivity as

$$t_\lambda = \frac{I_{\lambda ,L}}{I_{\lambda ,0}} = e^{- k_\lambda L} \tag{8}$$

The absorptivity is $a_\lambda = 1 - t_\lambda = 1 - e^{- k_\lambda L}$, and for gray gases, $a_\lambda = e_\lambda =$ emmissivity. If we considere both gas emission and the absortion effect, the intensity of the beam is attenuated due to absortion and is augmented due to gas emission along th distance. Asume a local thermodynamic equilibrium, absorption coefficient will equal emission coefficient, and the eq.(2) becomes.

$$dI_\lambda \left(x\right) = \left[- K_\lambda I_\lambda \left(x\right) + K_\lambda I_{b\lambda} \right] dx \tag{9}$$

where $K_\lambda I_{b\lambda}$ is intensity gained due to gas emission, $- KI_\lambda \left(x\right)$ is the intensity attenuated due to gas absorption. Performing integration and applying the boundary conditions, we obtain

$$I_\lambda \left(L\right) = I_{\lambda ,0} e^{- K_\lambda L} + I_{b\lambda} a_\lambda \tag{10}$$

In general, the absorption coefficient K_l is strongly dependen ton wavelength. If we use the average overall the wavelength of total properties, we obtain: $K_l = K, a = 1 - t, a = e, I_l = I,$

$$I(L) = I_0 e^{-KL} + e s T_g^4 \tag{11}$$

3.3. Radiation Exchange

The following shows how to determine radiation heat transfer between surfaces in an enclosure with radiation gases. Assume that there are *N* gray diffuse and isothermal surfaces. This implies that each surface at T_i has uniform radiosity J_i (emission plus reflection). Also we assume that radiation gases are gray gases at uniform temperature and pressure (emissivity=absorptivity) and have no scattering effect. Figure 1 shows an energy balance on surface *i*, and energy balance between surface *i* and the rest of enclosure surfaces *j* through gases.

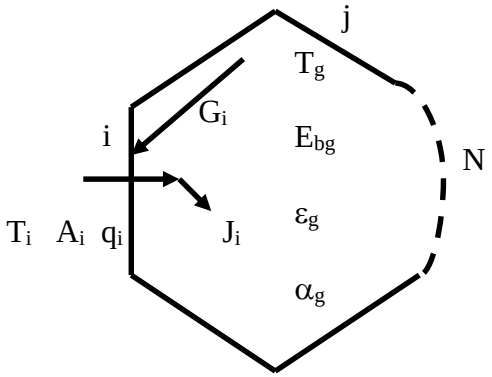

Figure 1. Radiation heat transfer through gases in an enclosure

As show in Figure 1, if we perform energy balance on surface i, net heat transfer rate = radiosity (energy out) – irradiation (energy in), we obtain,

$$q_i = A_i (J_i - G_i) \tag{12}$$

Performing energy balance between surface i and the rest of surfaces j through radiation gases,

$$q_i = \frac{J_i - E_{bg}}{\underbrace{\left(\frac{1}{A_i \varepsilon_{i,g}}\right)}_{\text{resistance due to gas emissivity}}} + \sum_{j=1}^{N} \frac{J_i - J_j}{\underbrace{\left(\frac{1}{A_i F_{ij}(1-\alpha_{ij,g})}\right)}_{\text{resistance due to view factor and gas absorptivity}}} \tag{13}$$

Since gas absorptivity + gas transmissivity = 1, therefore, $1 - a_{ij,g} = t_{ij,g} = e^{-kL}$, the eq. (13) can be write for a gray enclosure filled with a gray gas as,

$$q_i = \frac{J_i - E_{bg}}{\frac{1}{A_i e_{i,g}}} + \frac{J_i - J_j}{\frac{1}{A_i F_{ij}\left(t_{ij,g}\right)}} \tag{14}$$

3.4. Electric Network Analogy

The case of study of this work considers the system as a gray enclosure filled with a gray gas, i.e. a cavity in which one face is the zircaloy (at temperature T_1) and the rest are a refractory surfaces and inside they are steam water (a gray gas at temperature T_g). Figure 2 shows a cavity, a refractory surface R, and a gray gas, g, where each element is assumed to be at a uniform temperature T_1, T_R, and T_g.

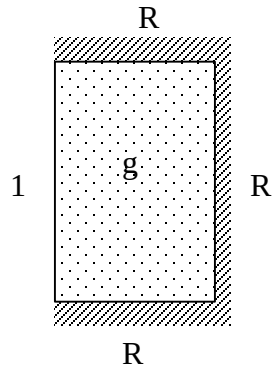

Figure 2. A gray enclosure filled with a gray gas.

Electric network analogy can be used to solve the radiation heat transfer problem, one may define the thermal resistance like the electrical resistance, and for this case we considered a gray enclosure filled with a gray gas.

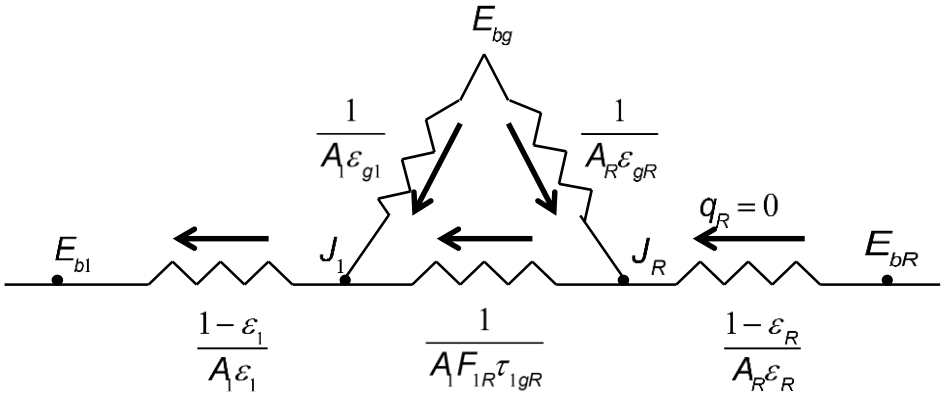

Figure 3. Electric network for a cavity filled with a gray gas

In order to determinate the radiation heat transfer between the surface and gas we resolved the electric network shown in the Figure 3 and we obtain,

$$q_{1g} = \frac{s\left(T_1^4 - T_g^4\right)}{\left(1 - e_1\right)\Big/ A_1 e_1 + 1\Big/\left\{A_1 e_{g1} + 1\Big/\left[1\Big/\left(A_R e_{gR}\right) + 1\Big/\left(A_1 F_{1R} t_{1gR}\right)\right]\right\}} \tag{15}$$

3. MATHEMATICAL MODEL

The system under consideration is depicted in Figure 4, which consists of an array of fuel cylinder (Figure 4(c)) bars, each coated with a cladding and a current of steam flowing outside the cylinders. In the same figure, we also show a representative array of the fuel rods where the initial and boundary-value problems for heat and mass transfer are to be solved. In this way, we can identify that the problem under study has a characteristic length of the order of P, that is, 16.2 mm, in contrast with the fuel assembly that is ten times larger (Figure 4(b)).

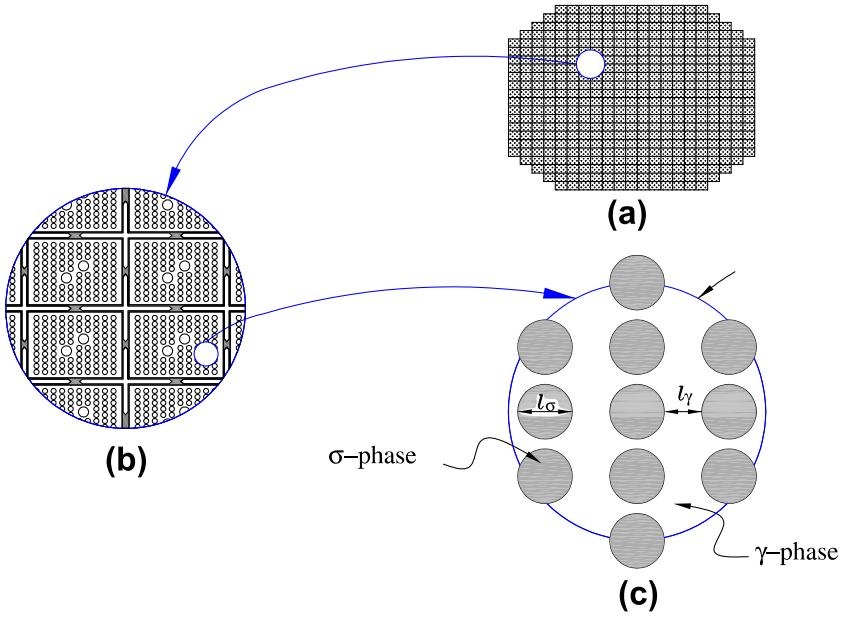

Figure 4. Characteristic lengths of the system. (a) Nuclear reactor core; (b) Fuel assembly; (c) Array of fuel rods.

The model is formed by power due to residual heat in the core reactor. The fuel rod temperature model considers radial nodes by each axial node that include fuel, gap and cladding. The hydrogen concentration is modeled with 2D axial and radial, which consider convection and diffusion transport phenomena. The flow is modeled with one-dimensional momentum balance, which considers driven force due to natural convection by two effects: hydrogen concentration and temperatures gradients. The energy balance in the nuclear reactor is a one-dimensional transient approximation. In addition, this model uses a set of empirical correlations the heat transfer coefficient in the convection natural range.

The fuel assembly temperature distribution was obtained considering eight radial nodes at each of the twelve axial nodes in the core. Two radial nodes are considered for the clad and the gap, two more nodes for the boundary condition evaluation and four nodes are considered for one equivalent fuel element. The transient temperature distribution in the fuel, initial and boundary conditions are given by:

$$(\rho Cp)_c \frac{\partial T_c}{\partial t} = k_c \frac{1}{r}\frac{\partial}{\partial r}\left(r\frac{\partial T_c}{\partial r}\right) + q'''(t) + E_i \tag{16}$$

$$(\rho Cp)_s \frac{\partial T_s}{\partial t} = k_s \frac{1}{r}\frac{\partial}{\partial r}\left(r\frac{\partial T_s}{\partial r}\right) - E_i \tag{17}$$

$$T(r,0) = T(r), \qquad \text{at} \qquad t = 0 \tag{18}$$

$$-k\frac{\partial T}{\partial r} = q'' + \Delta H_r(T)k(T)c_{H_2}, \qquad \text{at} \qquad A_i \tag{19}$$

$$\frac{\partial T}{\partial r} = 0, \qquad \text{at} \qquad r = r_0 \tag{20}$$

In these equations, the subscript c is used for the clad and s for the steam; r is the cylindrical radial coordinate, r_0 is the centroid of the fuel, and A_i is the interfacial area between fuel rod and fluid, $q'''(t) = P(t)/V_f$ at each axial node, P is given by Eq. (24), and the heat flux is given by:

$$q'' = H\left(T_m - T_{cl}\right) + q_{1g} \tag{21}$$

where T_m is the fluid temperature, T_{cl} is the clad temperature, H is the convective heat transfer coefficient, which given by [19] for natural convection. The term E_i is the interfacial term of the relation in the interface, and is given by:

$$E_i = m(T_f - T_c) \tag{22}$$

The closure relationship μ is given by [20]:

$$\frac{A_i m l_g^2}{k_s} = \frac{40a\left(a^2 + a + 1\right)k}{\left(1+5k\right) + a\left(2+k\right) + \left(a^4 + 2a^3 + 3a^2\right)\left(1 - k\right)} \tag{23}$$

where l_g represents the adjacent length between two rods of fuel, see Figure 4c, and a is the porosity. And $k = k_c / k_s$.

Evaluation of the heat generated in a reactor after shutdown is important for determining cooling requirements under normal conditions and accident consequences. Reactor shutdown heat

generation is the sum of heat produced from fission due to delayed neutron or photoneutron emissions, and decay of fission products fertile materials, and activation products. The heat decay level used in this work is given by [21]:

$$\frac{P}{P_0} = 0.066\left[(\tau - \tau_s)^{-0.2} - \tau^{-0.2}\right] \tag{24}$$

where P_0 is the steady-state power rate, $(\tau - \tau_s)$ is time after shutdown, and τ is the time after reactor startup. The heat of the reaction, which applies into Eq. (19) is given by:

$$\Delta Hr = -6.304940\times10^{2} + 2.996279\times10^{-2}T - 2.179432\times10^{-6}T^{2}, \quad \text{for} \quad 298.15\,K \le T < 1445.15\,K \tag{25}$$

$$\Delta Hr = -6.318406\times10^{2} + 4.755655\times10^{-2}T - 9.785421\times10^{-6}T^{2}, \quad \text{for} \quad 1445.15\,K \le T \le 2273.15\,K \tag{26}$$

The transition solid phase enthalpy is: $\Delta H_t = 8.4\ kJ/mol$ at 1445 *K*. The kinetics of the oxidation reaction is divided in three parts, in each one is involved a phase transition of the zirconium and zirconia from α to β and monoclinic to tetragonal and to cubic respectively. Correlations were obtained from experimental sets, over the temperature range 973 to 1873 K. Weight gain and many specimens for grow of ZrO_2 and $\alpha - Zr(O)$ were measured gravimetrically. These correlations are for temperature range of 973 K to 1873 K [22]:

$$K_T = 7.24\exp\left(\frac{-0.871\times10^{5}}{RT}\right) \tag{27}$$

$$K_{ox} = 2.80\times10^{-3}\exp\left(\frac{-0.840\times10^{5}}{RT}\right) \tag{28}$$

where K_T is the parabolic coefficient of total oxygen mass gain ($kg/m^2 s^{0.5}$), K_{ox} is the coefficient of oxide scale growth ($m/s^{0.5}$).

The mass transfer phenomena consider that the hydrogen generated diffuses in the coolant by convection and diffusion. Then, the governing equation and boundary conditions for mass transfer for hydrogen concentration (c_{H2}) are given by:

$$\frac{\partial c_{H_2}}{\partial t} + \frac{G_m}{\rho_m}\frac{\partial c_{H_2}}{\partial z} = D\left[\frac{1}{r}\frac{\partial}{\partial r}\left(r\frac{\partial c_{H_2}}{\partial r}\right) + \frac{\partial^2 c_{H_2}}{\partial z^2}\right] \tag{29}$$

$$-D\frac{\partial c_{H_2}}{\partial r} = k_r(T)c_{H_2} \qquad \text{at} \qquad A_i \tag{30}$$

$$\frac{\partial c_{H_2}}{\partial r} = 0\,, \qquad \text{at} \qquad D_h / 2 \tag{31}$$

$$c_{H_2} = c_0\,, \qquad \text{at} \qquad z = 0 \tag{32}$$

$$c_{H_2} = c_L\,, \qquad \text{at} \qquad z = L \tag{33}$$

where D is the diffusive coefficient, D_h is the hydraulic diameter, k_r reaction rate coefficient given by Eqs. (27) and (28), c_0 and c_L are constants. The hydrogen concentration at the initial time is: $c_{H_2} = f(t=0, r, z)$.

Balancing the gravity head available and the total loop pressure drop obtained by the momentum balance integration leads to the natural circulation model. The natural circulation model includes the pressure drops in the reactor core, in order to obtain the following momentum balance:

$$A_{x-s}\frac{dG_m}{dt} = \left(\sum_{i=1}^{n}\frac{l_i}{A_i}\right)^{-1}\left(-K_{eq}\frac{G_m^2}{\rho_m} - \Delta p_c\right) \tag{34}$$

where $\left(\sum l/A\right)$ is the inertial term, K_{eq} is the core loss coefficient, Δp_c is the core pressure drop, and Δp_g is the pressure drop due to gravity. The total core pressure drop is the sum of the frictional, acceleration and gravitational components:

$$-\Delta p_c = \sum_{j=1}^{n}\left[\frac{2C_{f0}G_m^2\Delta z}{D_h\rho_m} + G_m^2\left(\frac{1}{\rho_{m,j+1}} - \frac{1}{\rho_{m,j}}\right) + \bar{\rho}_{m,j}g\Delta z\right] \tag{35}$$

where *n* is the axial total cell in the core, j represents each axial cell in the core, C_{f0} is the single-phase friction factor, Δz is the core node length, ρ_m is the core density in each node, $\bar{\rho}_m$ is the core density using the equation of state

3.1. Boussinesq approximation

The phenomenon of free convection results from the fact that when the fluid is heated, the density decreases and the fluid rises. The phenomena of free convection also are due to hydrogen concentration gradients. The mathematical description of the system must take this essential feature of the phenomenon into account for this work. Then, the Boussinesq approximation for $\bar{\rho}_m$ of the Eq. (35) is given by [23].

$$\bar{\rho}_{m,j} = \rho_{m,j} - \rho_{m,j}\beta_j(T_{cl,j} - T_{m,j}) - \rho_{m,j}\gamma_j(c_{H2,j}^{cl} - c_{H2,j})\,, \qquad \text{for} \qquad j = 1,2,3,...,n \tag{36}$$

where the T_{cl} and $c_{H2,j}^{cl}$ are the temperature and concentration at the wall of the cladding fuel, T_m is the moderator temperature, and β is the volumetric expansion coefficient, which is defined by:

$$\beta_j = -\frac{1}{\rho_{m,j}}\left(\frac{\partial \rho_{m,j}}{\partial T}\right)_p, \qquad \text{for} \qquad j = 1,2,3,...,n \tag{37}$$

The mass transfer coefficient is analog of the coefficient β:

$$\gamma_j = -\frac{1}{\rho_{m,j}}\left(\frac{\partial \rho_{m,j}}{\partial c}\right)_{H2}, \qquad \text{for} \qquad j = 1,2,3,...,n \tag{38}$$

The last two terms of the Eq. (36) describe the buoyant force resulting from the temperature and concentration variation within the fluid, which are analyzed in this work.

4. NUMERICAL SOLUTION

Application of the control volume formulation enables the equations for each region (fuel, gap and clad) to be written as a single set of algebraic equations for the sweep in the radial direction in implicit scheme lead to:

$$a_j T_{i,j-1}^{t+\Delta t} + b_j T_{i,j}^{t+\Delta t} + c_j T_{i,j+1}^{t+\Delta t} = d_j \tag{39}$$

where $T_{j-1}^{t+\Delta t}$, $T_j^{t+\Delta t}$ and $T_{j+1}^{t+\Delta t}$ are unknowns, *a, b, c and d* are coefficients, which are computed at the time t. When these equations are put into a matrix form, the coefficient matrix is tridiagonal.

The numerical solution of the concentration model considers also the application of the control volume formulation, but in explicit scheme:

$$a_{i,j} C_{i,j-1}^{t+\Delta t} = b_{i,j} C_{i+1,j}^{t} + c_{i,j} C_{i,j}^{t} + d_{i,j} C_{i-1,j}^{t} + e_{i,j} C_{i,j-1}^{t} + f_{i,j} C_{i,j+1}^{t} \tag{40}$$

where a to f are coefficients. The energy balance is given by Eqs. (16) and (17). The momentum balance is given by Eq. (34); both are solved using the Euler method approximation.

The heat transfer processes are coupled with the mass transfer process through reaction rate and heat reaction at the interface, which are a function of the temperature. And the momentum transfer is coupled with mass transfer model with convection term. Thus, in this work the simultaneous transfer of momentum, heat and mass is considered.

A computer program was developed for analysis of transport process for radiation heat transfer effects during a severe accident and was implemented in FORTRAN on Windows platform with MS FORTRAN 4.0 compiler POWERSTATION Microsoft Corp.

5. NUMERICAL EXPERIMENT

The numerical experiments were performance in an averaging channel that represents a core reactor with the fuel rod with its gap and cladding and cooling steam of a BWR, in order to establish the importance of the effects of radiation heat in a severe accident scenario. The initial conditions of this scenario correspond to 100% of rated power, with scram of the reactor without cooling flow, i.e., without mitigation effects. The temperature of the fuel is incremented due to decay heat, which follows the transient behavior given by Eq. (24). Then, due to lack of cooling the fuel temperature increases. Eventually the temperature rise causes fuel cladding oxidation and hydrogen.

The transient behavior of the average cladding temperature with and without radiation heat effects is shown in Figure 5. In this figure temperature rise is lower than radiation heat effects. In this figure the average cladding temperature is defined as:

$$T_{av} = \frac{1}{V}\int_V T_{clad}\,dV \tag{41}$$

The transient behavior of the average concentration of hydrogen is presented in Figure 6. Clearly it can be observed that diffusion of hydrogen is slower regarding to radiation.

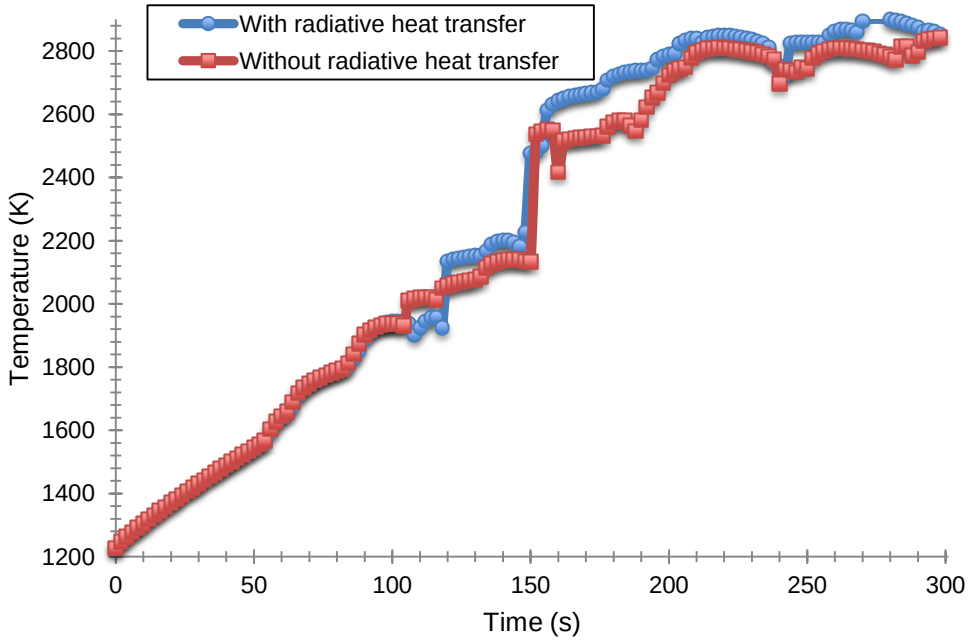

Figure 5. Transient comparison of average cladding temperatures.

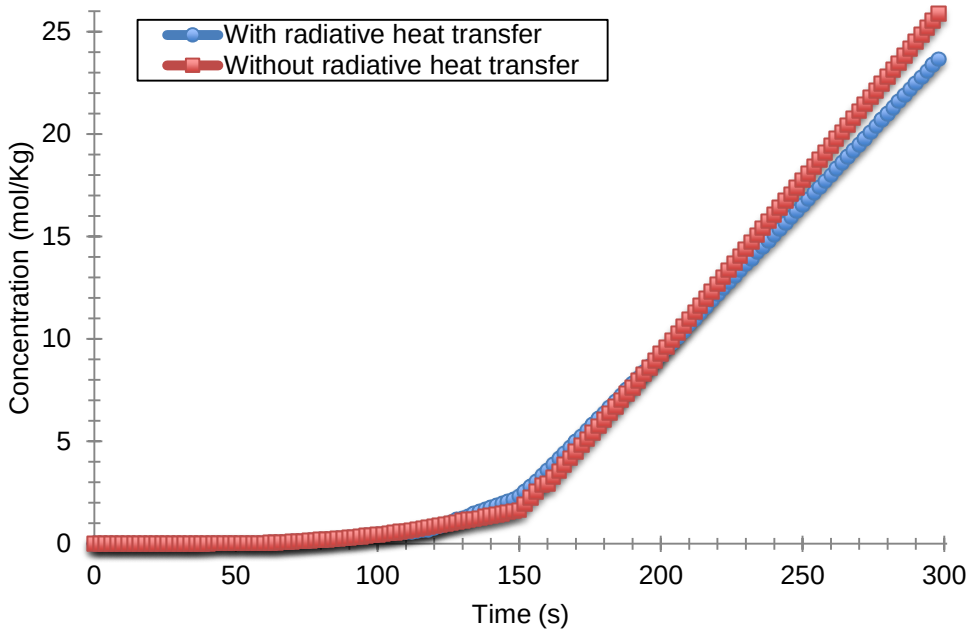

Figure 6. Transient comparison of average hydrogen concentration.

6. CONCLUSIONS

The aim of this work was to study the behavior of radiation heat transfer effects on the temporal evolution of the distributions of hydrogen concentration and temperature profiles in a fuel assembly where a stream of steam is flowing.

The mass transfer phenomenon considers that the hydrogen generated diffuses in the steam by convection and diffusion. Fuel rod cladding oxidation is then one of the key phenomena influencing the core behavior under high-temperature accident conditions. The heat transfer process in the fuel and thermo-hydraulics in the core assembly is described with a reduced order model. The Boussinesq approximation was applied in the momentum equations for multicomponent flow analysis that considers natural convection due to buoyancy forces, which is related with thermal and hydrogen concentration effects.

The heat transfer processes are coupled with the mass transfer process through reaction rate and heat reaction at the interface of the fuel, which are a function of the temperature. And the momentum transfer is coupled with mass transfer model with interface term. Thus, in this work the simultaneous transfer of momentum, heat and mass is considered.

In this work we carried out numerical simulations in an averaging channel that represents a core reactor with the fuel rod with its gap and cladding and cooling steam of a BWR. The results obtained in this work show the distributions of temperature and concentration in two-dimensional.

According with the results, the average cladding temperature is higher considering the effects of the radiation heat transfer in a participating medium, and the average concentration is lower because the hydrogen diffusion is slower regarding to those obtained without radiation heat transfer effects.

ACKNOWLEDGEMENTS

The authors acknowledge the support given by the Universidad Autónoma Metropolitana (UAM) through a scholarship at the Graduate Program in Energy and Environment at the UAM-Iztapalapa.

REFERENCES

1. D. R. Olander, "Materials chemistry and transport modeling for severe accident analyses in light-water reactors I: external cladding oxidation," *Nuclear Engineering and Design*, vol. 148, no. 2-3, pp. 253–271, 1994.
2. F. Fichot, B. Adroguer, A. Volchek, and Y. Zvonarev, "Advanced treatment of zircaloy cladding high-temperature oxidation in severe accident code calculations Part III. Verification against representative transient tests," *Nuclear Engineering and Design*, vol. 232, no. 1, pp. 97–109, 2004.
3. G. Schanz, B. Adroguer, and A. Volchek, "Advanced treatment of zircaloy cladding high-temperature oxidation in severe accident code calculations Part I. Experimental database and basic modeling," *Nuclear Engineering and Design*, vol. 232, no. 1, pp. 75–84, 2004.
4. C. Duriez, M. Steinbr¨uck, D. Ohai, T. Meleg, J. Birchley, and T. Haste, "Separate-effect tests on zirconium cladding degradation in air ingress situations," *Nuclear Engineering and Design*, vol. 239, no. 2, pp. 244–253, 2009.
5. M. Steinbrück, "Prototypical experiments relating to air oxidation of Zircaloy-4 at high temperatures," *Journal of Nuclear Materials*, vol. 392, no. 3, pp. 531–544, 2009.
6. E. Beuzet, J.-S. Lamy, A. Bretault, and E. Simoni, "Modelling of Zry-4 cladding oxidation by air, under severe accident conditions using the MAAP4 code," *Nuclear Engineering and Design*, vol. 241, no. 4, pp. 1217–1224, 2011.
7. X. Shi and X. Cao, "Study and assessment of Zry cladding oxidation model under severe accident in PWR," *In Proceedings of the Asia-Pacific Power and Energy Engineering Conference* (APPEEC '11), pp. 1–5,Wuhan, China, March 2011.
8. Erbacher, F.J., Leistikow, S., "A review of zircaloy fuel cladding behavior in a loss-of-coolant accident". *Kernforschungszentrum Karlsruhe*, KFK 3973, pp. 3–4, September 1985.
9. Xingwei, S., Xinrong, C., 2011. Study and assessment of Zry cladding oxidation model under severe accident in PWR. *In: Power and Energy Engineering Conference* (APPEEC) Asia-Pacific, pp. 1–5.
10. C.M. Allison, J.K. Hohorst, B.S. Allison, D. Konjarek, T. Bajs, R., Pericas and R., López, "Preliminary assessment of the possible BWR core/vessel damage states for Fukushima Daiichi station blackout scenarios using RELAP/SCDAPSIM," *Science and Technology of Nuclear Installations*, 2012.
11. Van Dorsselaere, J.P., Auvinen, A., Beraha, D., Chatelard P., Kljenak I., Miassoedov A., Paci S., Tromm T.W., Zeyen R., "The European research on severe accidents in generation 2 and 3 nuclear power plants," *Science and Technology of Nuclear Installations*, 2012.

12. G. Espinosa-Paredes, R. Camargo, A. Nuñez-Carrera, "Severe accident simulation of Laguna Verde Nuclear Power Plant," *Science and Technology of Nuclear Installations*, 2012.
13. R. Kapulla, G. Mignot, D. Paladino, "Large scale containment cooler performance experiments under accident conditions," *Science and Technology of Nuclear Installations*, 2012.
14. R.P. Martin, "An EMDAP paradigm for severe accident safety issue resolution," *Science and Technology of Nuclear Installations*, 2012.
15. A. Nunñez-Carrera, R. Camargo, G. Espinosa-Paredes, A. López-García, "Simulation of the lower head of boiling water reactor vessel in severe accident," *Science and Technology of Nuclear Installations*, 2012.
16. H. Romero-Paredes, F. J. Valdés-Parada, and G. Espinosa-Paredes, "Heat and Mass Transfer during Hydrogen Generation in an Array of Fuel Bars of a BWR Using a Periodic Unit Cell," *Science and Technology of Nuclear Installations*, 2012.
17. F.J. Valdés-Parada, H. Romero-Paredes, G. Espinosa-Paredes, "Numerical analysis of hydrogen generation in a BWR during a severe accident", *Chemical Engineering Research and Design*, **9**(1), (2013) 614–624
18. J. Chin Han, "Analytical Heat Transfer", CRC Press Taylor and Francis Group, 2012.
19. H.A. Mohammed, Y. K. Salman, "Heat transfer by natural convection from a uniformly heated vertical circular pipe with different entry restriction configurations," *Energy Conversion and Management*, 48, pp. 2244–2253, 2007.
20. Whitaker, S., 1999. The Method of Volume Averaging. Kluwer Academic Publishers, The Netherlands.
21. N. E. Todreas, M. S. kazimi "Nuclear Systems I: Thermal Hydraulic Fundamentals", Hemisphere Publishing Corporation, 1990.
22. S. Leistikow and G. Schanz, "Oxidation kinetics and related phenomena of zircaloy-4 fuel cladding exposed to high temperature steam and hydrogen-steam mixtures under PWR accident conditions," *Nuclear Engineering and Design*, 103, pp. 65-84, 1987.
23. R.B. Bird, W.E. Stewart, E.N. Lightfoot, "Transport phenomena", Second Edition, John Wiley and Sons, Inc., Phoenix, USA., 2002.